

Bulk superconductivity and disorder in single crystals of LaFePO

James G. Analytis¹, Jiun-Haw Chu¹, Ann S. Erickson¹, Chris Kucharczyk¹, Alessandro Serafin²,

Antony Carrington², Catherine Cox³, Susan M. Kauzlarich³, Håkon Hope³, I. R. Fisher¹

¹*Geballe Laboratory for Advanced Materials and Department of Applied Physics, Stanford University, CA 94305, USA.*

²*H. H. Wills Physics Laboratory, University of Bristol, 1 Tyndall Ave., Bristol BS8 1TL, UK and*

³*Department of Chemistry, University of California, Davis, California 95616, USA*

(Dated: May 28, 2018)

We have studied the intrinsic normal and superconducting properties of the oxypnictide LaFePO. These samples exhibit bulk superconductivity and the evidence suggests that stoichiometric LaFePO is indeed superconducting, in contrast to other reports. We find that superconductivity is independent of the interplane residual resistivity ρ_0 and discuss the implications of this on the nature of the superconducting order parameter. Finally we find that, unlike T_c , other properties in single-crystal LaFePO including the resistivity and magnetoresistance, can be very sensitive to disorder.

PACS numbers: 74.25.Fy, 74.25.Ha, 74.70.-b, 72.80.Ng

I. INTRODUCTION

High-temperature superconductivity in the iron-pnictides has recently attracted considerable attention because it is the first family of materials since the discovery of the cuprates to exhibit critical temperatures above 40K. However, in the initial flurry of activity, single-crystal measurements of the lower T_c analogue LaFePO have been somewhat overlooked. Early measurements of polycrystalline samples indicated T_c values in the range from 4 to 7 K,^{1,2,3,4,5} with F-substitution (i.e. electron doping)² or Ca-substitution (hole doping)³ modestly increasing T_c values. However, more recent measurements have queried whether the stoichiometric compound is actually superconducting, suggesting rather that oxygen deficiency plays a significant role.⁶ Initial single-crystal work revealed superconducting transitions in the resistivity and susceptibility, but not in the heat capacity, leading the authors to speculate that the superconductivity might be associated with an oxygen deficient surface layer, while the bulk remains metallic to the lowest temperatures.⁷ Given the close structural and electronic similarity to the parent compounds of the higher T_c oxyarsenides, it is particularly important that a clear picture of superconductivity in this lower- T_c analog is elucidated.

LaFePO is interesting for reasons other than this controversy. Because of its lower T_c and H_{c2} , quantum oscillations can be measured in relatively moderate fields.⁸ In addition, despite the appearance of a nearly-nested Fermi surface, LaFePO does not appear to exhibit any magnetism and so the properties of the *metallic* ground state of the pnictides can be examined in detail. In contrast LaFeAsO has a spin-density-wave ground state at low temperature and only exhibits superconductivity when doped, which naturally introduces disorder, inhibiting such detailed probes of the Fermiology.

In this paper we present results of heat capacity, magnetization, resistivity and magnetoresistance measurements of single-crystal samples of LaFePO. The evidence suggests that these samples are stoichiometric, and we report three major results. Firstly, we find that supercon-

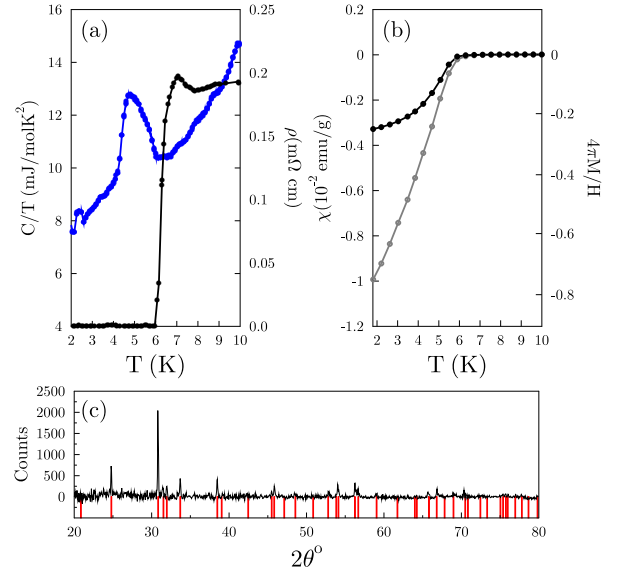


FIG. 1: (Color online)(a) Specific heat (left axis) of a mosaic of single-crystals and resistivity (right axis) of a single-crystal. The heat capacity anomaly corresponds to the disappearance of resistance. (b) The susceptibility of powdered LaFePO crystals measured in an applied field of 50 Oe following zero field cooling (ZFC) and field cooling (FC) cycles. (c) Powder x-ray diffraction pattern (black) of crystals taken from the same batch as in (b). All peaks can be indexed to the calculated pattern (red).

ductivity is present in the bulk of the material, contrary to the findings of some other authors.^{6,7} Second, we find the superconducting gap is uncorrelated with the interplane residual resistivity ρ_0 . If this quantity is representative of disorder, the lack of T_c suppression is consistent with *s*-wave superconductivity.¹¹ Finally, in contrast to the superconductivity itself, properties near T_c can vary greatly with disorder. We illustrate this with measurements of the magnetoresistance.

II. EXPERIMENT

Single-crystals of LaFePO were grown from a molten Sn flux, using conditions modified from the original work by Zimmer and coworkers.¹² Elemental and oxide precursors were placed in alumina crucibles and sealed in quartz tubes under a small partial pressure of argon. The growths were ramped up in temperature to 1190°C followed by a slow cool. We used either La₂O₃ or Fe₂O₃ to introduce oxygen into the melt. When La₂O₃ was used, the highest yield was obtained for a melt containing La:La₂O₃:Fe:P:Sn in the molar ratio 1:1:3:3:57, while with Fe₂O₃ the best yield was obtained from a combination La:Fe₂O₃:P:Sn in the molar ratio 3:1:2:24. The former method yielded our largest crystals (up to 0.7mm on a side) and with the highest RRR (residual resistivity ratio, $\rho(300K)/\rho(0)$), but the yield was very sensitive to the packing in the crucible, the temperature profile of the initial warm up, and the proportion of the other elements. The temperature was raised from room temperature to 1190°C in 6 hours, held for a further 6 hours and then lowered to 900°C at a rate of 4.8 °C/hour. Using Fe₂O₃ yielded crystals of the right phase more consistently, although smaller (typically 0.1-0.4mm) and with a lower RRR. In this case, optimal results were obtained by heating over the same amount of time, but the mixture was held at 1190°C for 18hrs, before cooling at 10 C/hour to 650°C. The remaining liquid was decanted at the base temperature using a centrifuge, and the crystals removed from the crucible. Excess Sn on the surface of the crystals was removed by etching in dilute HCl followed by an immediate rinse in methanol. Both methods resulted in multiphase growths, the principle second phase being LaFe₂P₂, which has the ThCr₂Si₂ structure. Care must be taken to distinguish these two phases.

Crystals grown using La₂O₃ precursor as described above had RRR values up to 85, $T_c \sim 5.9K$ and an interplane residual resistivity of $\rho_0 = 0.04m\Omega cm$. Crystals grown by this technique have been used for recent ARPES¹³ measurements while crystals grown using Fe₂O₃ were used to measure de Haas-van Alphen (dHvA) magnetization oscillations.⁸ The second method, using Fe₂O₃, with a melt composition much closer to that used in Reference 7, yielded crystals with a RRR ~ 25 , $T_c = 6.7K$ and an interplane residual resistivity of $\rho_0 = 0.18m\Omega cm$.

While optimizing the synthesis conditions, batches of crystals extracted from individual growths were checked by powder x-ray diffraction using an SSI XPERT diffractometer. Individual crystals were screened by measurement of the c-axis lattice parameter. A well-formed single crystal grown with La₂O₃ precursor and the melt composition and temperature profile that produced the highest quality crystals (as measured by the residual resistivity) was selected for X-ray study. A tin deposit on the crystal was removed by rinsing in a drop of 12 N HCl. A multiply-redundant MoK α data set of 1643 reflections ($2\theta_{max} = 63.9^\circ$) was measured on a Bruker Apex II

diffractometer. The crystal temperature was 90 ± 1 K. Data were corrected for absorption with the face-indexed procedure of SADABS9. The structure refined with SHELX¹⁰ to a standard R index of 0.0084, and a weighted R index of 0.02 for all 156 unique reflections. The oxygen occupancy is 100% within the statistical uncertainty of 1.8%. The crystals are tetragonal, space group *Pnmm*, with cell dimensions $a = 3.941 \pm 0.002$, $c = 8.507 \pm 0.005$.

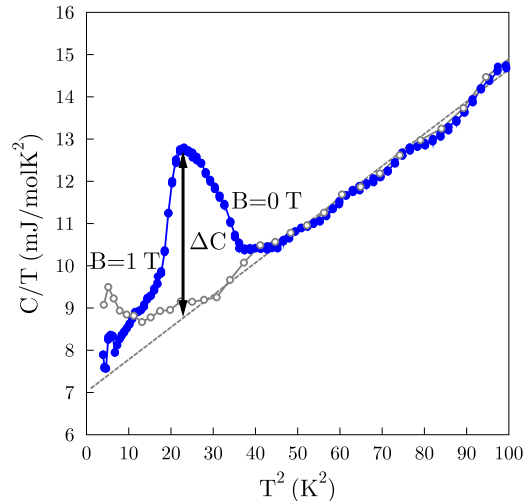


FIG. 2: (Color online) The specific heat C_p/T as a function of T^2 for a mosaic of LaFePO crystals taken in zero field (solid circles) and in an applied field of 1 T (open circles) with field oriented parallel to the *c*-axis. The dotted line indicates the linear fit as described in main text which extrapolates to a value of $\gamma \sim 7.0 \pm 0.2$ mJ/molK².

Inter-plane (*c*-axis, ρ_c) and in-plane (*ab*-plane, ρ_{ab}) resistivity measurements were made with a standard four-probe configuration and metallic contact was made using Epotek H20E paste. The paste was annealed in air at 200°C for 20 minutes. Inter-plane measurements were made on crystals as small as 0.15x0.1x0.02mm³ and in-plane measurements were made on larger crystals. However, the larger crystals tended to suffer from inhomogeneity (evidenced by a broad superconducting transition), and/or flux inclusions, and the *c*-axis data were generally better. Resistivity and heat capacity measurements were performed on a Quantum Design PPMS (14T). Due to the small size of the crystals, the heat capacity was measured for a mosaic of around 100 crystals grown from a melt containing La₂O₃, with a total mass of $800 \pm 50 \mu g$, each oriented such that the *ab*-plane was parallel to the platform. Crystals from a separate batch were powdered, half of which was checked for phase purity by powder x-ray diffraction (Figure 1 (c)). Susceptibility measurements were made for the other half of this powder sample using a Quantum Design MPMS 5 Superconducting Quantum Interference Device magnetometer

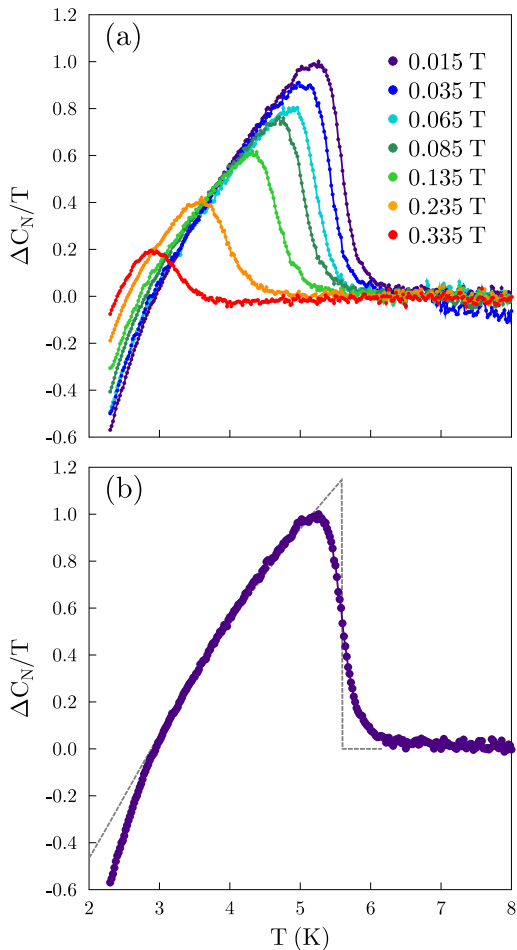


FIG. 3: Heat capacity data on a single-crystal ($\sim 5\mu\text{g}$) measured using the AC technique giving the relative change of the the heat capacity C from the normal state C_N (in arbitrary units), where $\Delta C = C - C_N$. In (a) we show the field dependence of the heat capacity anomaly, approximately agreeing with the suppression of T_c extracted from resistivity (see Figure 10). In (b) we show data fitted with weak-coupling BCS theory assuming an isotropic s -wave order parameter. The data agrees very well to the theory.

in a range of applied fields.

Measurements of heat capacity were also made on a single crystal using an AC method.¹⁴ The sample with dimensions $140 \times 220 \times 30 \mu\text{m}^3$ (with mass $\sim 5\mu\text{g}$) we attached with GE varnish to a $12\mu\text{m}$ diameter Chromel-Constantan thermocouple, and heated with light at a frequency of 16Hz. The size of the temperature oscillations is inversely proportional to the heat capacity of the sample plus the addenda (varnish plus thermocouple). Although with this method it is possible to measure a very small single-crystal it is not possible to determine the absolute value of the specific heat. The heat capacity was measured as a function of field from -0.4T to 1T with

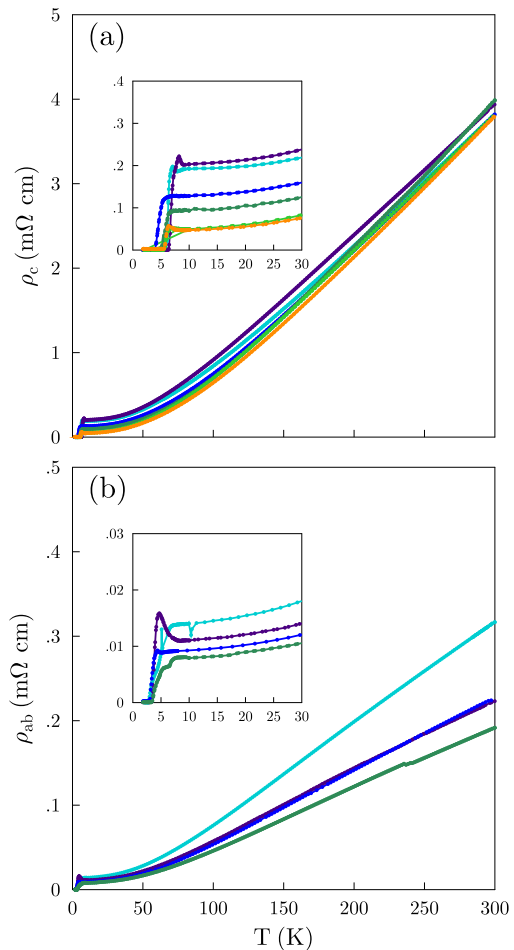


FIG. 4: (Color online) (a) Interlayer (c -axis) resistivity for LaFePO crystals grown using Fe_2O_3 (blue and green curves) and La_2O_3 (all other curves). The room temperature values are in approximate agreement for either method but the residual resistance ρ_0 shows significant variability (inset). (b) In-plane (ab -plane) resistivity. The room temperature value shows more variability than the interplane resistivity, primarily due to difficulties in finding homogeneous samples large enough to mount for in-plane measurements. This was often manifested in a broader superconducting transition (inset).

$B \parallel c$, in a 14T superconducting magnet. To account for the residual field in our magnet the actual field was determined from the field which produced the maximum field in a T_c versus H plot (the offset was 0.065 T).

III. RESULTS

Heat capacity data for the mosaic of single-crystal samples described above are shown in Figure 1(a) together with representative resistivity data for a single-crystal from a separate batch. The total heat capacity of this

mosaic is extremely small due to the small mass, making measurements of the relaxation time particularly challenging. Despite these difficulties, a clear superconducting anomaly is evident at 5.9 K, corresponding to the temperature at which the resistivity disappears. The superconducting state can be suppressed by an applied field greater than $\mu_0 H_{c2}$, leaving only the normal state contribution to the heat capacity (Figure 2). Data between approximately 5 and 10 K can be fitted using $C_v/T = \beta T^2 + \gamma$ where β and γ are the lattice and electronic heat capacity coefficients respectively. This yields an estimate of $\gamma = 7.0 \pm 0.2 \text{ mJ/molK}^2$ where one mole refers to the formula unit LaFePO. This value is similar to that obtained from values extracted by other authors for polycrystalline^{3,6} and single-crystal⁷ samples, though care should be taken on the definition of a mole (the value is doubled if one mole refers to the unit cell). Data on the low-temperature side of the superconducting transition are less reliable due to the small value of the heat capacity and the experimental difficulties measuring the relaxation time as described above. Due to these difficulties, the data does not appear to conserve entropy. Combined with the rounding of the superconducting anomaly seen in the data, it is difficult to obtain an accurate estimate of the heat capacity jump, but we can obtain a conservative lower bound by comparing the peak of the transition with the normal state extrapolation (vertical arrow in Figure 1). This results in an estimate of the normalized heat capacity jump $\Delta C/\gamma T_c \approx 0.6 \pm 0.2$, which is greater than Kamihara *et al.*'s estimate based on measurements of polycrystalline samples,² and is less than (about 40%) the BCS result $(\Delta C/\gamma T_c)_{\text{BCS}} = 1.43$. The actual value is likely somewhat larger than this lower bound. Susceptibility measurements for a sample consisting of several powdered single-crystals are shown in Figure 1 (b) for an applied field of 50 Oe following both zero field cooling (ZFC) and field cooling (FC) cycles. Perfect diamagnetism ($4\pi M/H = -1$, shown on the right axis in Figure 1b) corresponds to a value of $-1.32 \times 10^{-2} \text{ emu/g}$. Assuming that the particle size is larger than the penetration depth ($\sim 0.2 \mu\text{m}$ ¹⁷), the FC value ($\sim -0.32 \text{ emu/g}$) provides the better estimate of the superconducting volume fraction, giving a lower bound of approximately 24%. This likely substantially underestimates the actual value due to flux pinning effects.

Heat capacity data for a single crystal, obtained using the AC technique, are shown in Figure 3. For a field of $> 0.47 \text{ T}$ the superconducting anomaly was suppressed to below $T=2.3 \text{ K}$ so we used this data as an estimate of the normal state heat capacity C_N (including addenda), and subtracted this from the data in zero field. The superconducting anomaly is now clearly visible, with T_c (mid point of the increase in C of $T=5.6 \text{ K}$ and width (10-90%) of 0.4 K). In Figure 3 (a), we show the field dependence of the anomaly in C . The decrease in T_c corresponds to $dT_c/dH = 7.2 \pm 0.1 \text{ K/T}$. Also shown Figure 3 (b) is the temperature dependence calculated from the weak-coupling BCS theory assuming an isotropic s -wave order

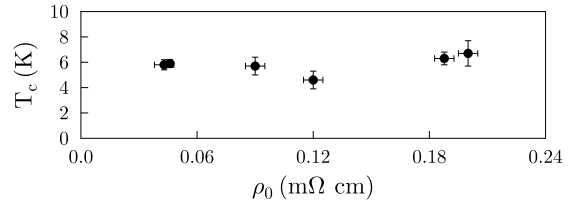


FIG. 5: Plot showing the dependence of the critical temperature T_c on the residual resistivity ρ_0 extracted from the low temperature normal state of LaFePO. The higher residual resistivities correspond to a ratio of the coherence length to mean free path $\xi_{ab}/l \sim 0.17 - 0.25$, and so a partial, systematic suppression in T_c is expected for an anisotropic order parameter.

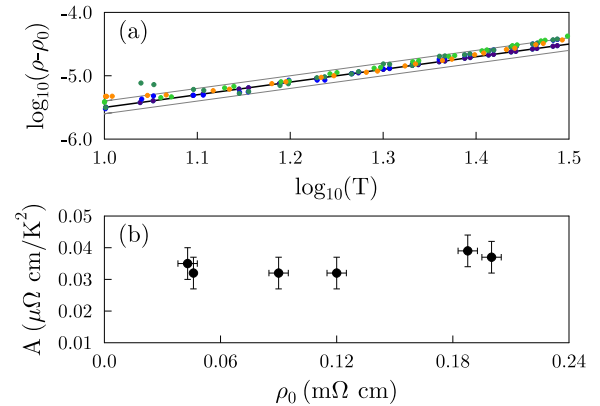


FIG. 6: (Color online) (a) c-axis resistivity data from Figure 3(a) replotted on a logarithmic scale. Plotted this way, all data fall on the same curve. The black line shows the value $A \sim 3.2 \times 10^{-5} \text{ m}\Omega\text{cm/K}^2$, while the grey lines illustrate our error bars in A . (b) The coefficient A extracted from fits of the resistivity data to $\rho = \rho_0 + AT^2$, which is independent of disorder.

parameter. Apart from the data very close to T_c or for $T < 2.8 \text{ K}$ the theory fits the data very well. The departure below $\sim 2.8 \text{ K}$ probably arises from the field dependence of the thermocouple thermopower and field dependence of the addenda which we have not attempted to correct for.

In the strong coupling Eliashberg theory the slope near T_c normalised to the jump at T_c $R = \frac{T_c}{\Delta C} \frac{\partial C}{\partial T} \big|_{T_c}$ is indicative of the coupling strength.¹⁵ The fact that our data fit well the weak coupling BCS form shows that LaFePO is in the weak coupling limit (note however this does not prove the order parameter is necessarily isotropic).

In Figure 4(a) we show the inter-plane (c-axis) resistivity ρ_c for five crystals grown from slightly different melt conditions. Absolute values of the room temperature resistivity are in excellent agreement, and the principal difference between the samples is the residual resistivity ρ_0 . A small upturn is seen in the resistivity of some but not all samples, just above T_c . T_c values are also in excel-

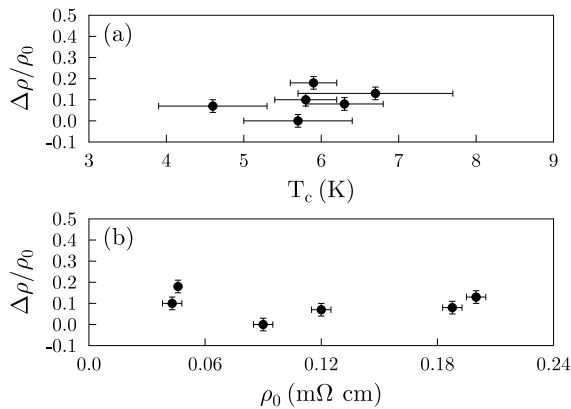


FIG. 7: (a) The magnitude of the interplane resistivity upturn $\Delta\rho_c = \rho_p - \rho_0$ normalized to the residual resistivity ρ_0 , where ρ_p is the peak resistivity of the upturn. There does not appear to be a correlation with T_c . (b) The magnitude of the interplane resistivity upturn $\Delta\rho_c$ as a function of the interplane residual resistivity ρ_0 , which also shows no correlation.

lent agreement, and show no correlation with the residual resistivity (see Figure 5). Similar data for in-plane resistivity measurements ρ_{ab} are shown in Figure 4(b). In contrast to the c -axis data, in-plane measurements tend to exhibit both broader transitions and also a wider variation in the absolute value of the resistivity. As described above, this difference can be ascribed to the use of larger crystals for the in-plane measurements, which are consequently more susceptible to defects, flux inclusions and, due to the malleability of the crystals, macroscopic distortion. The anisotropy of the interplane to in-plane resistivity ρ_c/ρ_{ab} is in the range from 13 to 17, in approximate agreement with band structure calculations.^{18,19,20}

Neglecting the low-temperature upturn seen in some samples, resistivity data below 25K can be well-fit by the standard Fermi liquid behavior, $\rho = \rho_0 + AT^2$, where ρ_0 is the residual resistivity.²¹ To confirm the reliability of this fitting, $\log(\rho - \rho_0)$ vs $\log(T)$ is shown in Figure 6(a) for the c -axis data, which reveals that each data set not only has a gradient of 2 ± 0.3 , but also falls on the same value of $A \sim 3.2 \pm 0.5 \times 10^{-5} \text{ m}\Omega\text{cm}/\text{K}^2$ (Figure 6(b)). We note in passing, that when A is combined with our value of γ we find a Kadowaki-Woods ratio of $A/\gamma^2 = 65 \pm 15 \times 10^{-5} \mu\Omega\text{cm}(\text{mol K}/\text{mJ})^2$.²²

As mentioned above, a small resistivity upturn is observed in some, but not all, samples just above T_c . This effect is seen for both current orientations (i.e. for ρ_{ab} and ρ_c). Significantly, the size of the upturn is not correlated with either T_c (Figure 7(a)), or with the absolute value of the residual resistivity ρ_0 extrapolated from higher temperatures (Figure 7(b)). We return to the field dependence and origin of this feature below.

Representative data showing the variation in the c -axis resistivity as a function of applied field at various temperatures are shown in Figure 8 for fields applied (a) parallel and (b) perpendicular to the c -axis. From

data like these we are able to extract $\mu_0 H_{c2}$, choosing for simplicity to define $\mu_0 H_{c2}$ in terms of the midpoint of the resistive transition, and using 10 and 90% of the transition to determine the error bars. Plotting $\mu_0 H_{c2}$ extracted in this manner, as shown in Figure 9 and extrapolating to $T = 0\text{K}$, we determine $\mu_0 H_{c2}^\perp(0) \sim 0.6T$ and $\mu_0 H_{c2}^\parallel(0) \sim 3.5T$, giving an anisotropy of ~ 6 . There is some variation in this value, perhaps due to the sensitivity of H_{c2}^\parallel to orientation, but most samples yield an anisotropy between 6 and 15, similar to that observed by other authors.⁷

The resistivity upturn which is observed in several samples is suppressed by an applied field, resulting in a pronounced “hump” feature in the magnetoresistance $\rho(H)$ for fields just above H_{c2} (see Figure 8). The magnitude of the resistivity upturn in zero field, and hence the associated negative magnetoresistance, varies between samples grown under different conditions, and to a lesser extent even between samples from the same batch. This variation is illustrated in Figure 10 which show representative c -axis and in-plane magnetoresistivity data for samples with small (panel (a)) and large (panel (b)) upturns respectively. The field is oriented parallel to the c -axis in both cases to allow direct comparison. For the sample shown in panel (a), the anomaly is suppressed by fields as small as $0.3T$, whereas for the sample shown in panel (b) it survives to fields of more than twice this value. In all cases, once the anomaly is completely suppressed, a positive magnetoresistance appears which is approximately linear with field in the high-field limit.

Significantly, the suppression of the resistivity upturn is strongly dependent on the orientation of the applied field with respect to the c -axis. For example, for the sample shown in Figure 11 (a-c), the resistivity upturn is suppressed for fields exceeding a modest 1 T when applied parallel to the c -axis, but is only suppressed for fields exceeding 12 T when directed perpendicular to the c -axis. Although the absolute values of the fields at which the resistivity upturn are suppressed vary between crystals depending on the magnitude of the zero-field upturn, this anisotropy is always observed. This anisotropy appears to mirror the anisotropy in $\mu_0 H_{c2}$, such that if magnetoresistance data for the two orientations are plotted as a function of field scaled by the appropriate value for $\mu_0 H_{c2}$ for that orientation, the data lie almost on top of each other (Figure 11 (d)). It is not clear whether this is coincidental, or reflects a deeper inter-relation between superconductivity and the origin of the resistivity upturn.

IV. DISCUSSION

The results summarized in Figure 1-3 provide the first evidence of superconductivity in single-crystals of stoichiometric LaFePO, manifested in a bulk thermodynamic transition in both the magnetization *and* the heat

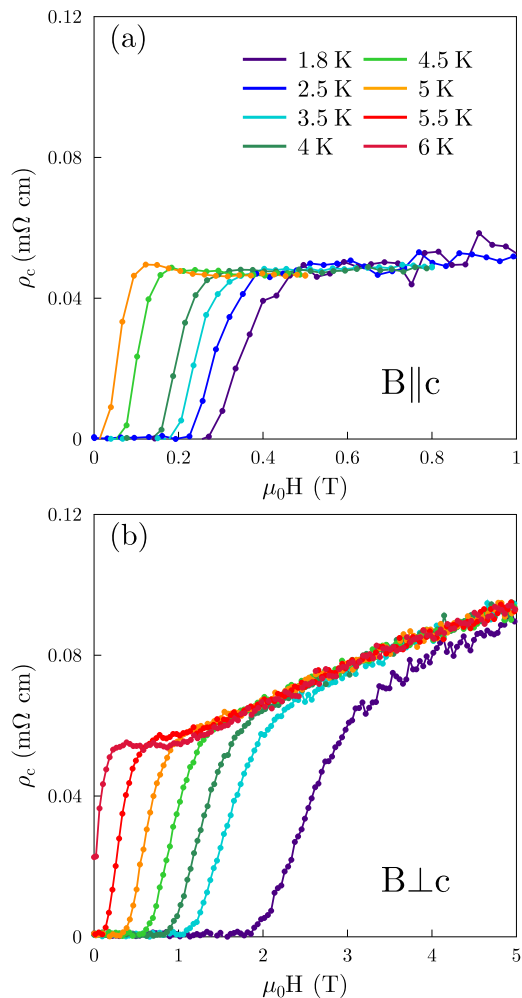


FIG. 8: (Color online) Interlayer (*c*-axis) resistivity as a function of magnetic field for (a) field parallel and (b) orthogonal to the *c*-axis for temperatures from 1.8 to 6.0 K (see legend in upper panel). The anisotropy in H_{c2} is approximately 6 in this case, though other samples show an anisotropy of up to 15.

capacity. In contrast, despite the observation of bulk superconductivity in polycrystalline samples by several other groups,^{3,4,5} McQueen et al. have recently suggested that the stoichiometric compound is actually non-superconducting, and that the onset of superconductivity is perhaps associated with the presence of oxygen deficiencies, among other possibilities.⁶ However, the absence of superconductivity in LaFePO would be surprising given that there is nothing anomalous in the density of states¹⁹ of the stoichiometric compound, no evidence of a competing phase transition, and doping with either holes or electrons results in superconductivity.¹ Using crystals grown by a similar technique to our own, Hamlin et al. observed a substantial diamagnetic susceptibility, but no anomaly in the heat capacity, causing them to suggest the possibility that their crystals have a thin surface

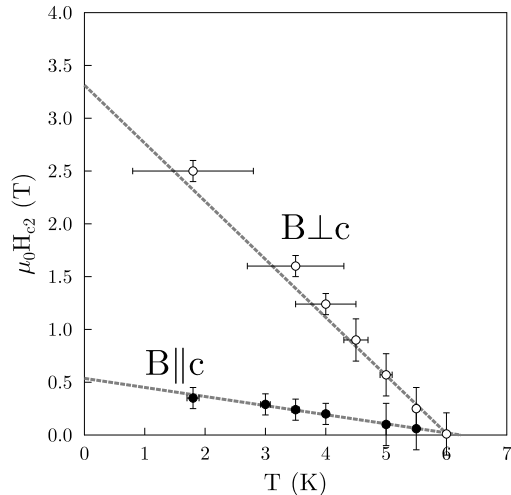


FIG. 9: The critical field $\mu_0 H_{c2}$ for fields oriented parallel (solid symbols) and perpendicular (open symbols) to the *c*-axis. Data points were determined from resistivity data as described in the main text. Error bars indicate 10 and 90 % of the superconducting transition.

layer of oxygen-deficient superconducting material surrounding a stoichiometric non-superconducting center.⁷ Refinements of single-crystal x-ray diffraction data for our crystals indicate full site occupancy, with a standard uncertainty in the oxygen content of only 1.8%. This is not the best probe of the oxygen content, but several other pieces of evidence suggest that oxygen deficiency, or at least variation in oxygen deficiency, does not play a significant role in these crystals. Specifically, neither the T^2 coefficient of the resistivity nor T_c itself (Figures 6 and 5 respectively), show any significant variation with the residual resistivity, in contrast to what would be expected if variation in the oxygen content were responsible for the different residual resistivity values if this were the principle source of disorder in these samples. Furthermore, these values do not depend on details of the synthesis conditions, including whether oxygen is introduced to the melt using Fe_2O_3 or La_2O_3 , and even the relative concentration of these precursors in the melt. These observations demonstrate that there is remarkably little variation in oxygen deficiency between crystals grown by this technique. In addition, the extremely high residual resistivity ratios, up to 85, indicate that the material is in fact exceptionally well-ordered. Finally, analysis of recent dHvA data taken for samples grown by this technique indicate that the electron and hole pockets are almost balanced, in agreement with the anticipated result for stoichiometric material,²³ with a mismatch that would correspond to a doping smaller than the error of our x-ray diffraction refinements.

Experiments involving annealing in an oxygen atmo-

sphere may be revealing, and though these are in progress one will always have the problem of establishing by how much the material has departed from perfect stoichiometry, which is a difficult measurement for such small crystals. Thus we cannot definitively prove the absence of oxygen deficiency from the present measurements, and in fact the breadth of the specific heat anomaly in Figure 1 may be indicative of slight variation in stoichiometry even within a single sample. However, given the small departure from stoichiometry that our errors allow, together with the above observations, it seems extremely unlikely that the stoichiometric compound is non-superconducting. Furthermore, the absence of other competing phases suggests that superconductivity is the natural low temperature ground state. In this case, the absence of a superconducting anomaly in the heat capacity data of Hamlin *et al.* likely reflects similar difficulties that we experienced in the measurement of such small sample masses. It is difficult to speculate on the reason for the absence of superconductivity in the polycrystalline samples of McQueen *et al.*⁶ but we note that the resistivity of those samples exhibits a substantial low-temperature upturn. We return to the possible significance of this below.

From the range and variety of samples measured in this work, we are also able to consider the role of disorder on the superconductivity of LaFePO. Even though these materials are anisotropic, the interplane transfer integral for the electron pockets is relatively large⁸ and so the interplane residual resistivity should be a good measure of the number of defects in a given crystal, though this argument is weaker for the hole pockets which have little warping in the k_z direction.²⁴ Assuming that this is the case, the plot of T_c vs ρ_0 , as shown in Figure 5 illustrates that T_c is, within our uncertainties, uncorrelated with disorder. For other high-temperature superconductors the absence of T_c suppression has been attributed to the smallness of the coherence length²⁶ ξ_{ab} . From the present measurements ξ_{ab} can be estimated from the relation $\mu_0 H_{c2}^\perp = \Phi_0 / 2\pi \xi_{ab}^2$, giving $\xi_{ab} \sim 0.03 \mu\text{m}$. The mean free path can be estimated from a quasi-two-dimensional Drude model $\sigma_{||} = (e^2/h) \times k_F l / c$, which yields a different conductivity for electron and hole pockets. Using the results of Reference 8, we estimate the electron and hole pockets to have a mean free path $l \sim 1700 \text{\AA}$ and $l \sim 1200 \text{\AA}$ respectively for the dirtiest samples, approximately in agreement with estimates from de Haas van Alphen oscillations.⁸ For the electron (hole) pockets this suggests the ratio ξ_{ab}/l has shifted from a value of ~ 0.04 (0.06) for the cleanest samples to ~ 0.17 (0.25) for the dirtiest samples. If the disorder were magnetic, a partial, systematic suppression of T_c should manifest for any pairing symmetry according to the relationship first calculated by Abrikosov and Gor'kov.^{25,26} Similarly, T_c for anisotropic d -wave or p -wave superconductors in the weak coupling limit should be suppressed due to the inevitable phase mixing of the order parameter, which should be noticeable by this value of ξ/l .^{24,26,27} Con-

versely, according to Anderson's theorem,¹¹ an s -wave superconductor should be robust against non-magnetic disorder due to the ability of the quasiparticle states to form time reversed pairs. The data in Figure 5 suggests that the predominant form of disorder is therefore non-magnetic. More importantly, if the dominant scattering is strong enough to scatter across the Brillouin zone, then this plot also illustrates that the order parameter mediating superconductivity is likely to be s -wave, an observation consistent with recent measurements of penetration depth¹⁷ on $\text{SmFeAsO}_{1-x}\text{F}_x$. However, if the scattering is small angle, or only occurs intra-Fermi surface, then an s -wave order parameter which reverses sign between Fermi surfaces centered at the Γ and M points may also be possible, as proposed by Mazin *et al.*²⁸ On the other hand, if the disorder is inhomogeneous on scales of order ξ , then it is possible than an anomalously clean path will yield a resistive transition T_c which is essentially disorder independent, though the superfluid density would be rapidly suppressed. This behavior may be evident in the heat capacity, and the breadth of the anomaly shown in Figure 1 may be indicative of just such inhomogeneity.²⁹ Naturally, the above discussion relies on the interplane resistivity being an accurate measure of the in-plane scattering rate, which may be true for the electron pockets due to their significant c -axis dispersion, but less likely for the hole pockets.

We now turn the discussion to the origin of the resistivity upturn observed in some crystals for temperatures just above T_c . Similar upturns are observed in several other classes of unconventional superconductors including many of the cuprates,³⁰ several organics^{31,32} and other polycrystalline oxy-arsenides.³³ However, in all these classes of compounds one observes an enhancement of the anomaly with an applied magnetic field, whereas in the present case we observe a suppression of the anomaly with field. In addition, we observe the upturn in some but not all of our samples, implying that this behavior is intimately linked with the presence of disorder. Finally, the anomaly is observed regardless of the current orientation, whereas in other correlated materials the effect is only observed when the current is passed along the c -axis.³⁰ In highly anisotropic materials with Josephson coupled planes, one expects dramatic differences in the behavior of each current orientation in field. Specifically, near T_c in-plane currents are dissipated by the motion of pancake vortices under the Lorentz force while interlayer currents are dissipated by the Josephson coupling between the layers, giving rise to a broad anomaly in ρ_c .³⁰ We thus rule out such coupling as the source of the anomaly.

Given the relatively large concentration of Fe in the melts used to grow these crystals, it is not unreasonable to suggest that the resistivity upturn might be associated with Kondo scattering from magnetic impurities. However, the strong anisotropy of the upturn's suppression with field, together with the fact that samples exhibiting the upturn do not show a dramatically suppressed

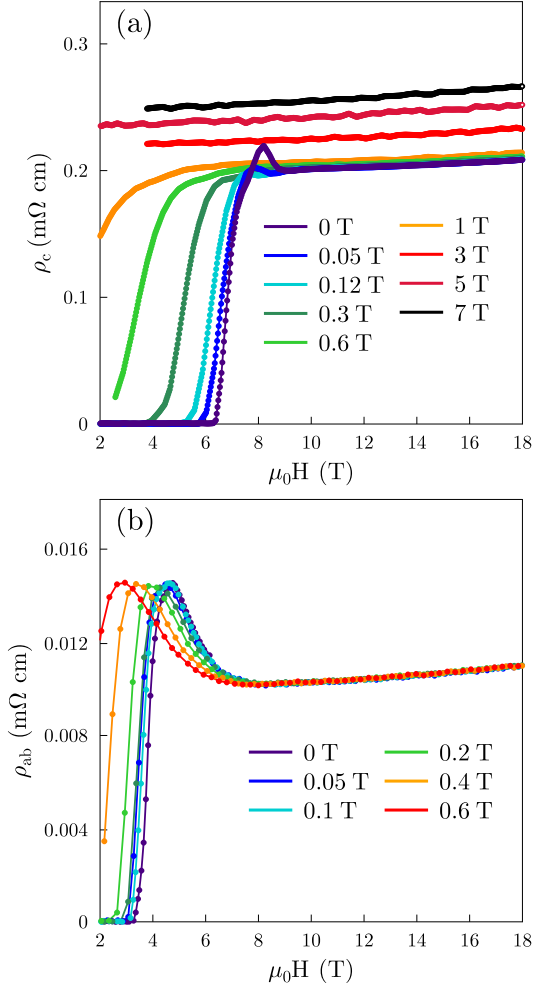


FIG. 10: (Color online) Temperature sweeps at constant field for field directed parallel to the c -axis illustrating the effect of applied fields on the resistivity upturn observed at low temperatures for some samples. In (a) we show the interplane resistivity for a sample with a small upturn and in (b) we show the in-plane resistivity for a sample with a pronounced up-turn. In both cases the anomaly is rapidly suppressed by magnetic field, though clearly the more pronounced the upturn, the higher the field required for the suppression.

T_c convincingly excludes this possibility. Another possible scenario for the origin of the resistivity anomaly is weak localization due to elastic scattering defects, possibly also explaining the rapid suppression of the anomaly with field. Furthermore, in quasi-two-dimensional systems, there can be a significant anisotropy in the field-induced suppression of weak localization.³⁴ However, the upturn does not scale with the residual resistivity ρ_0 (as shown in Figure 7 (b)), indicating that the effect does not correlate with the concentration of elastic scattering centers.

An intriguing alternative hypothesis for the origin of the resistivity anomaly is scattering from spin fluctua-

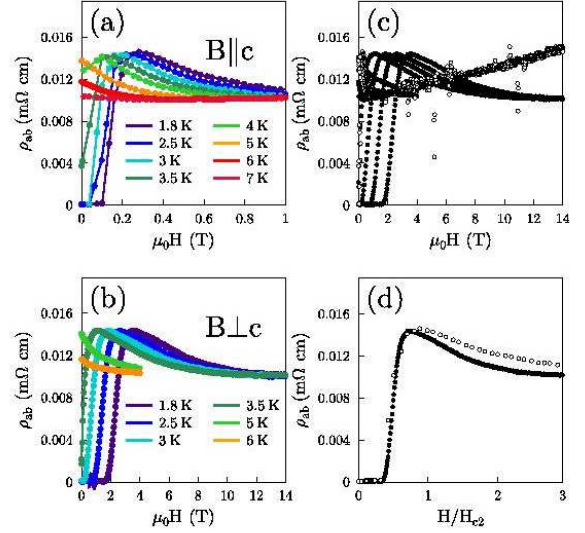


FIG. 11: (Color online) In-plane magnetoresistance for a sample with a pronounced upturn. At low fields the magnetoresistance is negative until the anomaly is completely suppressed. (a) illustrates the suppression when field is applied in-plane while (b) shows that the anomaly extends over a much wider field range when the field is applied orthogonal to the c -axis. (c) Illustrates both these data set on the same plot for direct comparison and (d) shows the data at 1.8 K scaled by $\mu_0 H_{c2}^{ab}$ for the in-plane data and $\mu_0 H_{c2}^c$ for the inter-plane data.

tions associated with a competing magnetic phase. Near perfect nesting of electron and hole pockets evidenced from dHvA measurements⁸ certainly raises the question as to whether the spin density wave (SDW) observed in the isolectronic compound LaFeAsO might be stabilized in LaFePO. In contrast, recent NMR results for $\text{La}_{0.87}\text{Ca}_{0.13}\text{FePO}$ indicate the presence of *ferromagnetic* fluctuations,³⁷ perhaps indicating that $q \sim 0$ nesting between concentric FS sheets dominates for such high doping levels. The same study also revealed anomalous behavior of $1/T_1 T$ below T_c for that material, indicating unusual spin dynamics in the superconducting state, though the origin of this effect is not yet clear. While the evidence points towards stoichiometric LaFePO being superconducting, one can speculate that, for example, magnetic impurities, or even disorder-induced variation in the Fe-P bond-length (which is believed to affect the magnitude of the Fe moment³⁶) might stabilize an incipient SDW in this material. However, there is no evidence for a magnetic or density wave transition in single-crystals of LaFePO, and T_c is uncorrelated with the magnitude of the resistivity upturn, at least for the range of values that we have observed. Hence, for such a scenario to be applicable, either the superconductivity must be insensitive to the presence/absence of magnetic fluctuations, or there must be some degree of inhomogeneity in the crystals, such that parts of the sample that suffer

such fluctuations are physically separate from the majority superconducting phase. Unfortunately, although this possibility is especially interesting due to the parallels to LaFeAsO, we cannot definitively establish whether it is appropriate from these measurements. Additional experiments are underway to determine the effect of stabilizing the SDW on the normal and superconducting states in this compound.

We note in closing that whatever the cause of the resistivity anomaly, it is reminiscent of an upturn seen by McQueen *et al.* for polycrystalline samples which had no superconducting transition.⁶ The residual resistivity ratio of those polycrystalline samples was nearly two orders of magnitude lower than that of the single-crystal samples described in this report, and the resistivity upturn was significant. This raises the possibility that the lack of superconductivity in those samples might not be due to differences in the oxygen content, but rather to a larger concentration of defects, potentially affecting a competing density wave ground state.

V. CONCLUSIONS

We have studied transport and thermal properties of single-crystals of LaFePO. These samples exhibit super-

conductivity, and the evidence suggests that stoichiometric LaFePO is indeed a bulk superconductor, in contrast to other reports. Furthermore we find that the superconducting gap is unrelated to non-magnetic disorder for values of $\xi/l \sim 0.2$ (assuming that disorder is proportional to the interplane resistivity). This result is consistent with an *s*-wave pairing symmetry, but is not definitive. Finally, we have investigated an anomalous low-temperature resistivity upturn that appears in some of our samples through detailed temperature and field studies. The feature is related to disorder, though the present measurements are insufficient to definitively establish the origin of this effect.

VI. ACKNOWLEDGEMENTS

We would like to thank Ross McDonald, Amalia Coldea, J. D. Fletcher, Scott Riggs, Stephen Kivelson, Doug Scalapino, Zach Fisk, Ben Powell, D. H. Lu, Ming Yi, Z. X. Shen and Theodore Geballe for useful comments on this work prior to publication. This work is supported by the Department of Energy, Office of Basic Energy Sciences under contract DE-AC02-76SF00515.

-
- ¹ Y. Kamihara *et al.*, Phys. Rev. B **77**, 214515 (2008)
 - ² Y. Kamihara *et al.*, J. Am. Chem. Soc. **128**, 10012 (2006)
 - ³ Y. Kohama *et al.*, arXiv:0806.3139 [cond-mat.supr-con]
 - ⁴ M. Tegel, I. Schellenberg, R. Pottgen and D. Johrendt, Z. Naturforsch., **63b**, 1057 (2008)
 - ⁵ C. Y. Liang, R. C. Che, H. X. Yang, H. F. Tian, R. J. Xiao, J. B. Lu, R. Li and J. Q. Li, Supercond. Sci. Technol. **20**, 687 (2007).
 - ⁶ T. M. McQueen *et al.*, Phys. Rev. B **78**, 024521 (2008)
 - ⁷ J.J. Hamlin *et al.*, J. Phys.: Condens. Matter **20**, 365220 (2008)
 - ⁸ A. Coldea *et al.*, arXiv:0807.4890 [cond-mat.supr-con]
 - ⁹ Sheldrick, G. M. (1996). SADABS. University of Göttingen
 - ¹⁰ Sheldrick, G. M. (2008). Acta Cryst. A **64**, 112122.
 - ¹¹ P.W. Anderson, J. Phys. Chem. Solids **11**, 26 (1959)
 - ¹² B. I. Zimmer *et al.*, J Alloys and Comp. **229**, 238 (1995)
 - ¹³ D. Lu, M. Yi, S.-K. Mo, A. S. Erickson, J. Analytis, J.-H. Chu, D. J. Singh, Z. Hussain, T. H. Geballe, I. R. Fisher, Z.-X. Shen, Nature **455**, 81 (2008)
 - ¹⁴ A. Carrington *et al.* PRB **55**, R8674 (1997)
 - ¹⁵ Atkis and Carbotte, Physica C **15**, 395 (1989)
 - ¹⁶ Zheng Li *et al.*, Phys. Rev. B **78**, 060504(R) (2008)
 - ¹⁷ L. Malone, J. D. Fletcher *et al.*, arXiv:0806.3908v1 [cond-mat.supr-con]
 - ¹⁸ D. J. Singh and M. H. Du, Phys. Rev. Lett. **100**, 237003 (2008)
 - ¹⁹ S. Lebegue, Phys. Rev. B **75**, 035110 (2007)
 - ²⁰ Y. Kamihara *et al.* Phys. Rev. B **77**, 214515 (2008), S. Lebegue, Phys. Rev. B **75**, 035110 (2007)
 - ²¹ The temperature of 10K was chosen as the lower bound of our Fermi liquid fit because the resistivity lower than this and near T_c is, for some samples, complicated by the presence of an up-turn.
 - ²² K. Kadowaki and S. B. Woods, Solid State Communications **58**, 507 (1986)
 - ²³ Due to electron counting arguments in combination with the Luttinger theorem the electron and hole FS pockets in the stoichiometric compound should enclose exactly equal volumes. Analysis of recent dHvA data taken for samples grown by the same technique described above indicate that the electron and hole pockets are almost perfectly balanced, in agreement with the anticipated result. Deviations from perfect charge balance in this analysis are slight, for instance corresponding to an oxygen deficiency of no more than 1.5%. Orbits associated with the small 3D electron pocket centered at the Z point of the Brillouin zone have not been convincingly observed, and this may account for some of the deficiency, though unlikely to account for all.⁸
 - ²⁴ B.J. Powell and R.H. McKenzie, Phys. Rev. B **69**, 024519 (2004)
 - ²⁵ A.A. Abrikosov and L.P. Gorkov, Sov. Phys. JETP **12**, 1243 (1961); A.I. Larkin, JETP Lett. **2**, 130 (1965)
 - ²⁶ R. J. Radtke, K. Levin, H. B. Schuttler, M. R. Norman, Phys. Rev. B **48**, R653, (1993)
 - ²⁷ A.P. MacKenzie *et al.*, Phys. Rev. Lett. **78**, 2271 (1997)
 - ²⁸ I. I. Mazin, D. J. Singh, M. D. Johannes, M. H. Du, Phys. Rev. Lett. **101**, 057003 (2008)
 - ²⁹ B. Spivak, P. Oretto, S. A. Kivelson, Phys. Rev. B **77**, 214523 (2008).
 - ³⁰ J. H. Cho *et al.*, Phys. Rev. B **50**, 6493 (1994)
 - ³¹ F. Zuo *et al.*, Phys. Rev. B **54**, 6107 (1996)
 - ³² H. Taniguchi, K. Kanoda, A. Kawamoto, Phys. Rev. B **67**,

- 014510 (2003)
- ³³ S. C. Riggs *et al.*, arXiv:0806.4011v1 [cond-mat.supr-con]
- ³⁴ C. Mauz, A. Rosch and P. Wolffe, Phys. Rev. B **56**, 10953 (1997)
- ³⁵ D. Graf *et al.*, Phys. Rev. B **69**, 125113 (2004)
- ³⁶ R. Che, R. Xiao, C. Liang, H. Yang, C. Ma, H. Shi and J. Li, Phys. Rev. B **77**, 184518 (2008).
- ³⁷ Y. Nakai, K. Ishida, Y. Kamihara, M. Hirano and H. Hosono, arXiv:0808.2293 [cond-mat.supr-con].